

Thermal Conductivity near H_{c2} for spin-triplet superconducting States with Line Nodes in Sr_2RuO_4

L. Tewordt and D. Fay

I. Institut für Theoretische Physik, Universität Hamburg, Jungiusstr. 9, 20355 Hamburg, Germany
(October 27, 2018)

We calculate the thermal conductivity κ in magnetic fields near H_{c2} for spin-triplet superconducting states with line nodes vertical and horizontal relative to the RuO_2 -planes. The method for calculating the Green's functions takes into account the spatial variation of the order parameter and superconducting flow for the Abrikosov vortex lattice. For in-plane magnetic field we obtain variations of the in-plane κ with two-fold symmetry as a function of rotation angle where the minima and maxima occur for field directions parallel and perpendicular to the heat flow. The amplitude of the variation decreases with increasing impurity scattering and temperature. At higher temperatures the minima and maxima of the variation are interchanged. Since the results for vertical and horizontal line nodes are almost the same we cannot say which of the two pairing models is more compatible with recent measurements of κ in Sr_2RuO_4 . The observed four-fold modulation of κ in $\text{YBa}_2\text{Cu}_3\text{O}_{7-\delta}$ is obtained for d-wave pairing by taking into account the particular shape of the Fermi surface and the finite temperature effect. The results for κ for the f-wave pairing state with horizontal line nodes disagree in some respects with the measurements on UPt_3 .

I. INTRODUCTION

The nature of the unconventional superconducting state in the layered ruthenate Sr_2RuO_4 ¹ is currently of great interest. The original proposal of a spin-triplet p-wave pairing state with broken time-reversal symmetry and a constant gap² has to be modified because recent specific heat³ and NMR relaxation rate⁴ experiments indicate the presence of line nodes in the superconducting gap. These results have led to the proposal of new spin-triplet pairing states including f-wave pairing states with line nodes vertical and horizontal with respect to the 2D-planes.⁵ A powerful tool for probing the anisotropic gap structure is the thermal conductivity κ in a magnetic field \mathbf{H} because κ is sensitive to the relative orientations of the heat current, the field, and the nodal directions of the gap. In fact, a modulation of κ of 4-fold symmetry with rotation of an in-plane magnetic field reflects the angular positions of the vertical line nodes for $d_{x^2-y^2}$ -wave pairing in $\text{YBa}_2\text{Cu}_3\text{O}_{7-\delta}$ (YBCO).⁶ The observed modulation of the heat current in UPt_3 with rotation of the in-plane magnetic field⁷ seems to be in accordance with a spin-triplet f-wave pairing state that has horizontal line nodes.⁸

Recently, the thermal conductivity κ in Sr_2RuO_4 has been measured in magnetic fields up to H_{c2} for field directions perpendicular and parallel to the ab-plane.^{9,10} For rotating in-plane field the in-plane κ exhibits small modulations of 2-fold and 4-fold symmetry with respect to the rotation angle α . Since the amplitudes of these variations are much smaller than the calculated amplitudes for f-wave pairing states with vertical line nodes,¹¹ it has been suggested that the actual pairing state in Sr_2RuO_4 has horizontal line nodes like those proposed in Ref. 5. Most theories of thermal conductivity in low fields¹² are based on the Doppler shift of the quasiparticle spectrum due to the circulating flow in an isolated vortex line.¹³ Here we shall employ a quite different approach valid for fields near H_{c2} in which both the effects of the supercurrent flow and the scattering of the quasiparticles by the spatial variation of the order parameter in the Abrikosov vortex lattice are taken into account.¹⁴

In Section II we present the theory and in Section III we discuss the results. The conclusions are contained in Section IV.

II. THEORY OF GREEN'S FUNCTIONS AND THERMAL CONDUCTIVITY IN HIGH MAGNETIC FIELDS

In the method of Ref. 14 the Gorkov integral equations for the normal and anomalous Green's functions G and F with kernels given by the Abrikosov vortex lattice function are solved by expanding all functions in Fourier series \mathbf{k} with respect to the sum of the spatial positions and in Fourier integrals \mathbf{p} with respect to the difference of the

spatial coordinates. In calculating the spatial averages it suffices to consider the $\mathbf{k} = 0$ Fourier component. The corresponding Green's functions are given by:¹⁴

$$G(\mathbf{p}, \omega) = [\tilde{\omega} - \xi + i\sqrt{\pi}\Delta^2 |f(\mathbf{p})|^2 (\Lambda/v \sin \theta) w(z)]^{-1}; \quad (1)$$

$$F(\mathbf{p}, \omega) = -i\sqrt{\pi}\Delta f(\mathbf{p}) (\Lambda/v \sin \theta) w(z) G(\mathbf{p}, \omega); \quad (2)$$

$$\Lambda = (2eH)^{-1/2}; \quad \Delta^2 = \overline{|\Delta(\mathbf{r})|^2}; \quad (3)$$

$$w(z) = \exp(-z^2) \operatorname{erfc}(-iz); \quad z = (\tilde{\omega} + \xi) \Lambda/v \sin \theta; \quad (4)$$

$$\tilde{\omega} = \omega + i\gamma; \quad \gamma = \Gamma [N(\omega)/N_0]^{-1}. \quad (5)$$

Here the applied field \mathbf{H} is along the c -axis, θ is the polar angle between \mathbf{p} and \mathbf{H} , v is the Fermi velocity in the ab -plane, and Γ is the normal-state impurity scattering rate. The spatial average Δ^2 of the absolute square of the Abrikosov vortex lattice function is approximately given for large κ by the relations¹⁴

$$(\Delta\Lambda/v)^2 = (H_{c2} - H)/6\beta_A H; \quad (\Lambda/v)^2 = (H_{c2}/H) [6\Delta_0^2]^{-1}. \quad (6)$$

Here, $\beta_A = \langle |\Delta|^4 \rangle / (\langle |\Delta|^2 \rangle)^2$ is the Abrikosov parameter and Δ_0 is the BCS gap parameter. For $\theta \rightarrow 0$ the argument z in Eq. (4) becomes very large and $w(z) \sim i/\sqrt{\pi}z$ which yields according to Eqs. (1) and (2) the ordinary Green's functions G and F for a gap $\Delta f(\mathbf{p})$ where $f(\mathbf{p})$ gives the \mathbf{p} -dependence. It should be pointed out that the self-energy term proportional to $iw(z)$ in Eq. (1) yields an imaginary part that corresponds to quasiparticle scattering by the vortex cores. For a field \mathbf{H} in the ab -plane with angle α between \mathbf{H} and the a -axis one has to make the following replacements in Eqs. (1) - (5):

$$\sin \theta \longrightarrow [\sin^2 \theta \sin^2(\phi - \alpha) + (v'/v)^2 \cos^2 \theta]^{1/2}; \quad (\alpha = \angle(\mathbf{H}, \mathbf{a})). \quad (7)$$

Here ϕ is the azimuthal angle of \mathbf{p} in the ab -plane and v' is the Fermi velocity parallel to the c -axis.

We use the general Kubo formula for the electronic thermal conductivity of strong-coupling superconductors¹⁵ and insert the Green's functions given in Eqs. (1) and (2). For simplicity we consider the 2D-case where \mathbf{p} lies in the ab -plane and the polar angle $\theta = \pi/2$. The integral over energy ξ is carried out by the method of residues (see Appendix C of Ref. 15) and yields the following result for κ_{xx} ($x = \hat{\mathbf{a}}$) for \mathbf{H} in the ab -plane:

$$\begin{aligned} \kappa_{xx} &= \frac{\pi N_0 v^2}{8T^2} \int_0^\infty d\omega \omega^2 \operatorname{sech}^2(\omega/2T) \int_0^{2\pi} \frac{d\phi}{2\pi} \frac{2 \cos^2 \phi}{\operatorname{Im} \xi_0} \\ &\times \frac{[1 - \pi(\Delta\Lambda/v)^2 |f(\phi)|^2 [\sin(\phi - \alpha)]^{-2} |w(z_0)|^2]}{|1 + 2(\Delta\Lambda/v)^2 |f(\phi)|^2 [\sin(\phi - \alpha)]^{-2} [1 + i\sqrt{\pi}z_0 w(z_0)]|^2}, \end{aligned} \quad (8)$$

where

$$z_0 = 2(\omega + i\gamma)(\Lambda/v) [\sin(\phi - \alpha)]^{-1} + i\sqrt{\pi}(\Delta\Lambda/v)^2 |f(\phi)|^2 [\sin(\phi - \alpha)]^{-2} w(z_0); \quad (9)$$

$$z_0 = (\omega + i\gamma + \xi_0)(\Lambda/v) [\sin(\phi - \alpha)]^{-1}. \quad (10)$$

Here ξ_0 is the position of the pole of G in the upper half complex ξ -plane which is determined by the transcendental equation (9). For very low temperatures it is a good approximation to take the integrand of the ϕ -integral in Eq. (8) in the limit $\omega \rightarrow 0$. Then the solution of Eq. (9) for z_0 becomes purely imaginary: $z_0 = ix_0$. By using the boundaries for the w -function at imaginary arguments one obtains the estimate¹⁶

$$x_0 = [2\gamma(\Lambda/v) + \beta] / \sin(\phi - \alpha); \quad \operatorname{Im} \xi_0 = \gamma + \beta(v/\Lambda), \quad (11)$$

where

$$\begin{aligned} \beta &= 2(\Delta\Lambda/v)^2 |f(\phi)|^2 \{ [4(\gamma\Lambda/v)^2 + 4(\Delta\Lambda/v)^2 |f(\phi)|^2 + \eta \sin^2(\phi - \alpha)]^{1/2} \\ &\quad + 2(\gamma\Lambda/v) \}^{-1}; \quad (4/\pi \leq \eta \leq 2). \end{aligned} \quad (12)$$

Then the ratio of κ_{xx} to the normal thermal conductivity κ_n is approximately given by

$$\begin{aligned} \frac{\kappa_{xx}}{\kappa_n} &= \int_0^{2\pi} \frac{d\phi}{2\pi} 2 \cos^2(\phi) \frac{\Gamma(\Lambda/v)}{[(\gamma\Lambda/v) + \beta]} [1 - (\Delta\Lambda/v)^{-2} |f(\phi)|^{-2} \beta^2] \\ &\times |1 + 2[\sin(\phi - \alpha)]^{-2} \{ (\Delta\Lambda/v)^2 |f(\phi)|^2 - \beta[\beta + 2(\gamma\Lambda/v)] \}|^{-2}. \end{aligned} \quad (13)$$

III. RESULTS FOR THE FIELD DEPENDENCE OF THE THERMAL CONDUCTIVITY FOR VERTICAL AND HORIZONTAL LINE NODES

We consider first the f-wave pairing state with vertical nodes at $\phi = \pm\pi/4$ and $\pm 3\pi/4$:⁵

$$\mathbf{d}(\mathbf{p}) = \Delta \hat{\mathbf{z}} (p_x + ip_y)(p_x^2 - p_y^2); \quad |f(\phi)|^2 = [\cos(2\phi)]^2. \quad (14)$$

In Fig. 1 (a) and (b) we have plotted our results for κ_{xx}/κ_n versus H/H_{c2} for $\Gamma/\Delta_0=0.5$ (0.2) and $\beta_A = 1.2$. Here we have used the relationships (6) connecting $(\Delta\Lambda/v)^2$ and $(\Lambda/v)^2$ to the ratio H/H_{c2} . The upper solid curves in Fig. 1 refer to the case $\mathbf{H} \parallel \hat{\mathbf{c}}$ which, according to Eq. (7), is obtained from Eq. (13) by replacing $\sin(\phi - \alpha)$ by $\sin\theta$ with $\theta = \pi/2$. The lower dashed curves show the case $\mathbf{H} \parallel \hat{\mathbf{a}}$, i.e., $\alpha = 0$. The solid curve in Fig. 1(a) increases almost linearly with H and agrees roughly with the data for perpendicular field shown in Fig. 1(a) of Ref. 9 at the lowest temperature. The solid curve in Fig. 1(b) for $\Gamma/\Delta_0 = 0.2$ disagrees with the data because of its upward curvature. The dashed curves both exhibit an upward curvature near H_{c2} which is however stronger in Fig. 1(b). Fig. 1(b) is in fact in better agreement with the data for parallel field shown in Fig. 1(b) of Ref. 9 due to the rapid increase of the thermal conductivity as H approaches H_{c2} .

We next consider the angular variation of the thermal conductivity in a parallel field. In Fig. 2(a) we show an example of κ_{xx}/κ_n vs the angle α between \mathbf{H} and the a-axis for $(\Delta\Lambda/v)=0.2$ and $\Gamma/\Delta_0 = 0.1$. The angular variation is seen to exhibit two-fold symmetry proportional to $\cos(2\alpha)$ with the minimum at $\alpha = 0$ where \mathbf{H} is parallel to the heat current and the maximum at $\alpha = \pi/2$. This behavior can be explained as an effect of the density of states which has a minimum for quasiparticles travelling parallel to the field and a maximum for quasiparticles moving perpendicular to the field.¹⁴ In fact, the expression $|\dots|^2$ in the denominators of equations (8) and (13) corresponds to $|N(\phi, \alpha)|^2$. In Fig. 3(a) we show the relative amplitude $\Delta\kappa = 2[\kappa(\alpha = \pi/2) - \kappa(\alpha = 0)]/[\kappa(\pi/2) + \kappa(0)]$ for $\Gamma/\Delta_0 = 0.1$ (solid curve) and 0.5 (dashed curve) vs H/H_{c2} . One sees that this amplitude becomes small for $H/H_{c2} \rightarrow 1$ and that it decreases with increasing impurity scattering rate Γ/Δ_0 . However, even for $\Gamma/\Delta_0 = 0.5$, the amplitudes are still larger percentages of κ than those shown in Fig. 2(b) of Ref. 9.

We have also considered the case where the heat current is in the direction $\phi_\kappa = \pi/4$ corresponding to the data for $\mathbf{q} \parallel [110]$ shown in Fig. 2(a) of Ref. 9. Then the directional factor $2\cos^2(\phi)$ in Eq. (13) has to be replaced by $2\cos^2(\phi - \pi/4) = 1 + \sin(2\phi)$. As an example we show in Fig. 2(a) κ_s/κ_n vs α for $\Delta\Lambda/v=0.2$ and $\Gamma/\Delta_0 = 0.1$. We see again the two-fold symmetry with the minimum occurring at $\alpha = \pi/4$, i.e., for \mathbf{H} parallel to the heat current \mathbf{q} , and the maximum at $\alpha = 3\pi/4$. This behavior is basically in agreement with the data in Fig. 2(a) of Ref. 9. However, at higher fields for $\Delta\Lambda/v=0.1$ (see Fig. 2(b)), a small local maximum occurs at $\alpha = \pi/4$ while a large maximum remains at $\alpha = 3\pi/4$. The occurrence of a local maximum and two neighboring minima is plausible since the quasiparticles are now travelling mainly along the node of the gap where the effect of the field on the density of states vanishes. This behavior seems to differ from the data in Fig. 2(a) of Ref. 9 at higher fields where a small component of 4-fold symmetry with minimum for $\mathbf{H} \parallel \mathbf{q}$ has been extracted (see Fig. 3 of Ref. 9). The order of magnitude of the relative amplitudes of the calculated oscillations for the heat current along the node of the gap is about the same as that shown in Fig. 3(a) where the heat current is directed along the antinode of the gap.

In Fig. 2(b) we have plotted our results for κ_s/κ_n vs α for the case where the factor $2\cos^2(\phi)$ in Eq. (13) has been replaced with 1. The resulting curve is seen to have 4-fold symmetry in α with minima at $\alpha = 0$ and $\alpha = \pi/2$ and maxima at $\alpha = \pi/4$ and $\alpha = 3\pi/4$. This form is similar to the 4-fold symmetry of κ observed experimentally in YBCO.⁶ The explanation may be the following: According to the theory of thermal conductivity,¹⁵ the conductivity κ_{ii} along axis i contains the factor v_i^2 where v_i is the component of the Fermi velocity along the i -axis. For a circular Fermi line this yields a factor proportional to $\cos^2(\phi - \phi_i)$. However, for YBCO the Fermi line is roughly a square and thus the component v_b along the b -axis is approximately constant along each side of the square. It is interesting that the data for Sr_2RuO_4 yield a small component of 4-fold symmetry which is similar to that shown in Fig. 2(b). This has been attributed however to the 4-fold anisotropy of H_{c2} .⁹ For lower fields we find an interchange of the maxima and minima of the 4-fold variation which is in agreement with the results in Ref. 11 (see Fig. 2(a)).

We turn now to the f-wave pairing state with vertical nodes where the term $(p_x^2 - p_y^2)$ in Eq. (14) is replaced by $p_x p_y$ and thus the squared amplitude $[\cos(2\phi)]^2$ in Eq. (14) is replaced by $[\sin(2\phi)]^2$.⁵ The resulting thermal conductivity is simply obtained from Eq. (13) for state (14) by making a variable transformation $\phi = \phi' - \pi/4$ in the ϕ -integral which yields the new field direction angle $\alpha' = \alpha + \pi/4$ and the heat current direction $\phi_\kappa = \pi/4$. Thus we obtain for the new state the same function of angle α' as the function of α in Fig. 2(a) (solid curve) shifted by $\pi/4$. Vice versa, for the heat current along the node of the old state the variable transformation $\phi = \phi' + \pi/4$ yields for the new state the same functions of the field angle $\alpha' = \alpha - \pi/4$ as in Fig. 2(a) (dash-dot curve) shifted by $-\pi/4$ where the heat current is now along $\phi_\kappa = 0$. The latter form of $\kappa(\alpha)$ agrees with that which has been obtained by the Doppler shift method for low fields in Ref. 11.

The authors of Ref. 9 suggested that a superconducting state with horizontal line nodes is a better candidate for explaining their thermal conductivity data. We therefore now consider the state⁵

$$\mathbf{d}(\mathbf{p}) = \Delta \hat{\mathbf{z}}(p_x + ip_y)[\cos(cp_z) + a_0]; \quad |f|^2 = [\cos(cp_z) + a_0]^2. \quad (15)$$

where $a_0 \leq 1$. Now the expression for κ_{xx}/κ_n in Eq. (13) has to be integrated over p_z . This leads to an additional integral over the new variable $\theta = cp_z$ from $-\pi$ to $+\pi$ of the expression in Eq. (13) with the squared gap amplitude replaced with $|f|^2 = (\cos(\theta) + a_0)^2$. For $\mathbf{H} \parallel \hat{\mathbf{c}}$ the terms $\sin(\phi - \alpha)$ in equations (12) and (13) have to be replaced by 1 which yields for $a_0 = 0$ the same result for κ_{xx}/κ_n as that for state (14). For \mathbf{H} lying in the ab-plane one has to carry out the double integral over θ and ϕ . In Fig. 4(a) we show κ_{xx}/κ_n vs H/H_{c2} for $\mathbf{H} \parallel \hat{\mathbf{a}}$ and parameter values $\Gamma/\Delta_0=0.5$ (0.1) and $\beta_A = 1.2$. The results are seen to be very similar to the dashed curves in Figs. 1(a) and 1(b) for the state (14). The modulation of κ_{xx}/κ_n with rotation angle α has two-fold symmetry with a minimum at $\alpha = 0$ and a maximum at $\alpha = \pi/2$ as can be seen in Fig. 4(b). The plots of κ_{xx}/κ_n vs α are very similar to those for state (14) (see Fig. 2(a), solid curve). In Fig. 3(b) we show our results for the relative amplitudes of the modulations for impurity scattering $\Gamma/\Delta_0=0.5$ and 0.1. These are nearly the same as those for state (14) shown in Fig. 3(a). The main difference between the states with horizontal and vertical line nodes is that, for the former states, the two-fold modulation of κ with rotation angle α of the in-plane field is always the same function relative to the direction of the heat current while, for the latter states, the modulation depends somewhat on the direction of the heat current relative to the vertical nodes (see Figs. 2(a) and 2(b)). This can be seen from Eq. (13) with the variable transformation $\phi = \phi' - \phi_\kappa$ for the heat current in the direction ϕ_κ which leads to the same function of the new rotation angle $\alpha' = \alpha + \phi_\kappa$ since $|f|^2 = \cos^2 \theta$ does not depend on ϕ . Thus we see that our results for states with horizontal nodes, as well as for states with vertical nodes, agree roughly with the observed thermal conductivity data. This is because the minimum of κ in Figs. 2(a) and 2(b) of Ref. 9 for heat current $\mathbf{q} \parallel [110]$ and $\mathbf{q} \parallel [100]$ occurs in both cases for $\mathbf{H} \parallel \mathbf{q}$.

We have also calculated the thermal conductivity for the following f-wave pairing state with horizontal line nodes which has been proposed for UPt₃:⁸

$$\mathbf{d}(\mathbf{p}) = (3\sqrt{3}/2)\Delta \hat{\mathbf{z}} p_z(p_x + ip_y)^2; \quad |f|^2 = (27/4) \cos^2 \theta (1 - \cos^2 \theta)^2. \quad (16)$$

The corresponding expression for κ_{bb}/κ_n is obtained from Eq. (13) by replacing the directional terms $\sin(\phi - \alpha)$ due to the field by the expressions in Eq. (7) with $\mathbf{v}'=\mathbf{v}$. The directional terms $|f|^2$ due to the squared gap amplitude are given now by Eq. (16). Additionally, the heat flow directional term $2 \cos^2 \phi$ in Eq. (13) is replaced by $3 \sin^2 \theta \sin^2 \phi$ for heat flow along the b-axis. The integrations over the polar angle θ and the azimuthal angle ϕ yield the variation of κ_{bb} vs the rotation angle α of \mathbf{H} in the ab-plane shown in Fig. 4(b). One sees that the modulation of $\kappa_{bb}(\alpha)$ has two-fold symmetry in α with a minimum at $\mathbf{H} \parallel \hat{\mathbf{b}} \parallel \mathbf{q}$ (\mathbf{q} is the direction of the heat flow) and a maximum at $\mathbf{H} \parallel \hat{\mathbf{a}}$. These results are contrary to the two-fold variation of κ observed in UPt₃ which shows a maximum for the field parallel to the heat flow.⁷ In Fig. 4(a) we show the dependence of κ_{bb} on H/H_{c2} for $\alpha = \pi/2$, i.e., $\mathbf{H} \parallel \mathbf{q} \parallel \hat{\mathbf{b}}$. One sees that κ_{bb} exhibits a strong upward curvature for small impurity scattering rate $\Gamma/\Delta_0 = 0.1$ while it becomes approximately linear in H for the larger scattering rate $\Gamma/\Delta_0 = 0.5$. According to the measurements of κ for UPt₃, the thermal conductivity κ_{bb} for the configuration $\mathbf{H} \parallel \mathbf{q} \parallel \hat{\mathbf{b}}$ increases almost linearly with H while, for the configuration $\mathbf{H} \parallel \mathbf{q} \parallel \hat{\mathbf{c}}$, κ_{cc} exhibits a steep increase as H tends to H_{c2} .⁷ Therefore we have also calculated κ_{cc} for $\mathbf{H} \parallel \mathbf{q} \parallel \hat{\mathbf{c}}$ and find surprisingly nearly the same field dependence as for κ_{bb} , i.e., in both cases κ is linear in H or increases steeply at H_{c2} . Thus we see that both our results for the field dependence of κ for $\mathbf{H} \parallel \hat{\mathbf{b}}$ and $\mathbf{H} \parallel \hat{\mathbf{c}}$, and the variation of $\kappa(\alpha)$ with the in-plane field rotation angle α are in disagreement with the measurements on UPt₃.⁷

Finally we discuss the ω -dependence of the integrand of Eq. (8) which determines the temperature dependence of the thermal conductivity. It is now necessary to solve Eq. (9) for z_0 as a function of ω and to integrate the resulting expression in Eq. (8) over ϕ . In Fig. 5(a) we have plotted the result (without the factor $\omega^2 \text{sech}^2(\omega/2T)$) vs $\Omega = \omega/\Delta$ for the state (14) at field directions $\alpha = 0$ and $\alpha = \pi/2$ for parameter values $\Delta\Lambda/v = 0.6$ and $\Gamma/\Delta_0 = 0.2$. The results for $\omega = 0$ agree with those obtained previously from Eq. (13). Most interesting is the result that the curves for $\alpha = 0$ and $\pi/2$ in Fig.5(a) cross each other at about $\Omega \simeq 0.7$ which means that for higher frequencies the former minimum of the integrand of κ_{xx} becomes a maximum and vice versa. This leads to a reduction of the field modulation at finite temperatures due to the factor $\omega^2 \text{sech}^2(\omega/2T)$ in the integrand of Eq. (8). In Fig. 5(b) we show our result for the temperature dependence of the relative amplitude $\Delta\kappa$ which is obtained by carrying out the ω -integrals in Eq. (8) with the integrands shown in Fig. 5(a). One recognizes that $\Delta\kappa$ decreases rapidly with increasing T/T_C and becomes small of the order of a few percent at the experimental values of T/T_C .⁹ Furthermore note that $\Delta\kappa$ even becomes negative in the temperature range between $T/T_C \simeq 0.25$ and 0.75 which means that the minimum and maximum are interchanged.

We have also calculated the frequency dependence of the integrand of κ_{xx} in Eq. (8) with the factor $2 \cos^2 \phi$ replaced by 1 which yields the 4-fold variation of $\kappa(\alpha)$ discussed above. For lower fields, or larger $\Delta\Lambda/v$, the maximum and

minimum of $\kappa(\alpha)$ occur, for $\omega = 0$, at field directions $\alpha = 0$ and $\alpha = \pi/4$, respectively. In Fig. 6 we show the curves $\kappa(\Omega)$ for $\alpha = 0$ and $\alpha = \pi/4$ for the same parameter values as in Fig. 5(a). Note that the curves cross each other for increasing frequency at a much lower frequency ($\Omega \simeq 0.3$) than in Fig. 5(a). This means that the maxima and minima of $\kappa(\alpha)$ are interchanged at a much lower temperature than that in Fig. 5(b). This is in agreement with the measurements on YBCO.⁶

IV. CONCLUSIONS

In summary, we have calculated the in-plane thermal conductivity κ near H_{c2} for different spin-triplet pairing states with line nodes in the superconducting gap which are directed perpendicular (vertical) and parallel (horizontal) to the ab-plane. For fields along the c-axis, κ increases approximately linearly with increasing field, while, for fields parallel to the ab-plane, κ exhibits an upward curvature as H approaches H_{c2} . For rotating in-plane magnetic field we obtain variations $\kappa(\alpha)$ of two-fold symmetry in the rotation angle α where the minimum and maximum occur for fields parallel and perpendicular to the heat flow. The relative amplitude $\Delta\kappa$ of the modulation decreases with increasing field, impurity scattering, and temperature. At higher temperatures $\Delta\kappa$ even changes sign indicating that the minimum and maximum of $\kappa(\alpha)$ are interchanged. Since all these results are nearly the same for the spin-triplet pairing models with line nodes vertical or horizontal to the RuO_2 planes, we cannot decide which one of the proposed models is more compatible with the recent data for Sr_2RuO_4 .^{9,10} The smallness of the observed variations of the in-plane κ for rotating in-plane field may well be accounted for by finite temperature effects. The only marked difference between our results for these two types of states is that for horizontal nodes the variation $\kappa(\alpha)$ always has the same form relative to the direction of the heat current while, for vertical nodes $\kappa(\alpha)$ is somewhat different for the heat current in the direction of an antinode or a node. For the heat current in the direction of a vertical node $\kappa(\alpha)$ shows a 2-fold symmetric modulation for lower fields (see the dash-dot curve in Fig. 2(a)). A similar form has been obtained in Ref. 11 for the state with squared amplitude $\sin^2(2\phi)$. We have shown in Section III that, for this state, the dash-dot curve in Fig. 2(a) is shifted by $-\pi/4$. For higher fields this modulation $\kappa(\alpha)$ develops some structure for field directions near $\alpha = \pi/4$ corresponding to the direction of the node (see the solid curve in Fig. 2(b)). Therefore we suggest more accurate measurements of $\kappa(\alpha)$ for different directions of the heat flow which could distinguish between the two types of pairing states. It would also be interesting to measure $\kappa(\alpha)$ at higher temperatures to see whether the predicted interchange of minima and maxima actually takes place.

No significant anisotropy in the inter-plane κ of Sr_2RuO_4 was observed for rotating in-plane field, perhaps indicating the existence of horizontal line nodes.¹⁰ In fact, for the states (15) and (16) with horizontal line nodes, κ_{cc} along the c-axis actually does not depend on the in-plane rotation angle α .

The f-wave pairing state with horizontal line nodes, which has been discussed for Sr_2RuO_4 , has also been proposed for UPt_3 .⁸ We have calculated κ_s with the help of the three-dimensional \mathbf{p} -integral and find that, for relative orientations $\mathbf{H} \parallel \mathbf{q} \parallel \hat{\mathbf{b}}$ as well as $\mathbf{H} \parallel \mathbf{q} \parallel \hat{\mathbf{c}}$, the field dependence of κ_s is nearly the same: it exhibits a steep upward curvature near H_{c2} for low impurity scattering rate Γ/Δ_0 while it becomes more linear for larger values of Γ/Δ_0 . These results disagree with measurements in UPt_3 where κ is found to be almost linear in H for the configuration $\mathbf{H} \parallel \mathbf{q} \parallel \hat{\mathbf{b}}$ while it increases steeply near H_{c2} for $\mathbf{H} \parallel \mathbf{q} \parallel \hat{\mathbf{c}}$.⁷ For rotation of \mathbf{H} in the ab-plane we obtain a modulation $\kappa(\alpha)$ of two-fold symmetry in the angle α with a minimum for $\mathbf{H} \parallel \hat{\mathbf{b}}$ and a maximum for $\mathbf{H} \parallel \hat{\mathbf{a}}$. This result is in agreement with that obtained by the Doppler shift method for low fields.⁸ However, these results are contrary to the observed two-fold variation of $\kappa(\alpha)$ in UPt_3 which has a maximum for the field parallel to the heat flow.⁷ Since these measurements were carried out at higher temperatures it may be that the interchange of maximum and minimum is due to the finite temperature effect. However, the disagreement between theory and experiment discussed above casts some doubt on the validity of this f-wave pairing model for UPt_3 .

Our calculation of κ for the f-wave pairing state with vertical line nodes (squared gap amplitude $\cos^2(2\phi)$) also applies to the $d_{x^2-y^2}$ -wave pairing state which is widely believed to be realized in the high- T_C cuprates. It is interesting that we obtain agreement with the observed four-fold symmetric variation $\kappa(\alpha)$ in YBCO⁶ if we neglect the directional factor arising from the squared component of the Fermi velocity in the direction of the heat flow. This approximation might be valid for the nearly square Fermi surface of YCBO because the Fermi velocity is almost constant on each side of the square. Our result that, for lower fields, the minima and maxima in $\kappa(\alpha)$ are interchanged is a problem that also occurs in the Doppler shift method at lower fields.¹¹ Here again, the finite frequency behavior, as seen in Fig. 6, and consequently the finite temperature effect calculated at the end of Section III, are responsible for the interchange of minima and maxima in the 4-fold variation $\kappa(\alpha)$ of the thermal conductivity which leads to agreement with the measurements on YBCO.⁶ In general, this interchange of maxima and minima is quite sensitive to the strength of the magnetic field and to the temperature.

Resolution of the remaining discrepancies between experiment and theory will require more measurements of the

thermal conductivity, in particular, for different directions of the heat flow. It should be pointed out that we have made some approximations in our theory of thermal conductivity¹⁵ near H_{c2} .¹⁴ First, we have neglected the small contributions of higher Landau levels N to the Abrikosov order parameter which occur for spin-triplet pairing.¹⁷ Second, we have neglected higher order Fourier coefficients of the Green's functions with respect to wave vectors \mathbf{k} of the reciprocal Abrikosov vortex lattice¹⁴ which become more and more important as the applied field is decreased. At fields near H_{c1} the complementary method of the Doppler effect for a single vortex becomes more appropriate, however, there the scattering of quasiparticles by a vortex core is neglected whereas it is taken into account in an average way by our method.

ACKNOWLEDGMENTS

We would like to thank T. Dahm for helpful advice and fruitful discussions.

-
- ¹ Y. Maeno, et al., Nature (London) **372**, 532 (1994).
² T. M. Rice and M. Sigrist, J. Phys. Condens. Matter **7**, L643 (1995).
³ S. NishiZaki, Y. Maeno, and Z. Mao, J. Low Temp. Phys. **117**, 1581 (1999); J. Phys. Soc. Jpn. **69**, 572 (2000).
⁴ K. Ishida et al., Phys. Rev. Lett. **84**, 5387 (2000).
⁵ Y. Hasegawa, K. Machida, and M. Ozaki, J. Phys. Soc. Jpn. **69**, 336 (2000).
⁶ H. Aubin, K. Behnia, M. Ribault, R. Gagnon, and L. Taillefer, Phys. Rev. Lett. **78**, 2624 (1997).
⁷ H. Suderow, H. Aubin, K. Behnia, and A. Huxley, Phys. Lett. **A234**, 64 (1997); H. Suderow, J. P. Brison, A. Huxley, and J. Flouquet, J. Low Temp. Phys. **108**, 11 (1997).
⁸ H. Won and K. Maki, Europhys. Lett. **52**, 1427 (2000).
⁹ K. Izawa et al., Phys. Rev. Lett. **86**, 2653 (2001).
¹⁰ M. A. Tanatar et al., Phys. Rev. Lett. **86**, 2649 (2001).
¹¹ T. Dahm, H. Won, and K. Maki, cond-mat/0006301.
¹² C. Kübert, and P. J. Hirschfeld, Phys. Rev. Lett. **80**, 4963 (1998).
¹³ G. E. Volovik, JETP Lett. **58**, 469 (1993).
¹⁴ U. Brandt, W. Pesch, and L. Tewordt, Z. Phys. (Lpz) **201**, 209 (1967).
¹⁵ V. Ambegaokar and L. Tewordt Phys. Rev. **134**, A805 (1964).
¹⁶ U. Brandt, Dr.rer.nat thesis (Hamburg, 1969).
¹⁷ K. Scharnberg and R. A. Klemm, Phys. Rev. B **22**, 5233 (1980).

FIGURE CAPTIONS

1. Thermal conductivity κ_s/κ_n vs applied field H/H_{c2} at $T=0$ for vertical line nodes (state 14) for \mathbf{H} parallel to the c -axis (solid curves) and \mathbf{H} parallel to the a -axis (dashed curves) for different impurity scattering parameters: (a) $\Gamma/\Delta_0=0.5$; (b) $\Gamma/\Delta_0=0.2$. The Abrikosov parameter is taken as $\beta_A=1.2$.

2. κ_s/κ_n vs $\alpha = \angle(\mathbf{H}, \mathbf{a})$ for in-plane field rotation at $T=0$ for state (14) with vertical nodes and impurity scattering rate $\Gamma/\Delta_0=0.1$. (a) Heat current \mathbf{q} in the direction of a vertical antinode (solid curve), \mathbf{q} in the direction of a vertical node (dash-dot curve), and no directional factor for \mathbf{q} (dashed curve), all for gap parameter $\Delta\Lambda/v=0.2$; (b) \mathbf{q} in the direction of a node (solid curve), and no directional factor for \mathbf{q} (dashed curve), both for $\Delta\Lambda/v=0.1$.

3. Relative amplitude $\Delta\kappa$ of the variation of $\kappa(\alpha)$ for rotating in-plane fields vs H/H_{c2} at $T=0$. (a) State (14) with vertical nodes and $\Gamma/\Delta_0=0.1$ (solid curve) and $\Gamma/\Delta_0=0.5$ (dashed curve). (b) State (15) with horizontal line nodes and $\Gamma/\Delta_0=0.1$ (solid curve) and $\Gamma/\Delta_0=0.5$ (dashed curve).

4. Magnetic field dependence of κ_S for horizontal line nodes at $T=0$. (a) κ_s/κ_n vs H/H_{c2} for state (15) with $\mathbf{H} \parallel \mathbf{q} \parallel \hat{\mathbf{a}}$ (dashed curves), and for state (16) with $\mathbf{H} \parallel \mathbf{q} \parallel \hat{\mathbf{b}}$ (solid curves), for $\delta = \Gamma/\Delta_0=0.1$ and 0.5 ; (b) κ_s/κ_n vs $\alpha = \angle(\mathbf{H}, \mathbf{a})$ for state (15) with $\mathbf{q} \parallel \hat{\mathbf{a}}$ (solid curve), and for state (16) with $\mathbf{q} \parallel \hat{\mathbf{b}}$ (dashed curve), for parameter values $\Delta\Lambda/v=0.2$ and $\Gamma/\Delta_0=0.1$.

5. (a) Integrand in Eq. (8) for κ_s/κ_n (without the factor $\omega^2 \text{sech}^2(\omega/2T)$) vs reduced frequency $\Omega = \omega/\Delta$ for state (14) and gap parameter $\Delta\Lambda/v=0.6$, for field direction $\alpha = 0$ (solid curve) and $\alpha = \pi/2$ (dashed curve). The impurity scattering rate is $\Gamma/\Delta_0=0.2$. (b) Relative amplitude $\Delta\kappa$ of the variation of $\kappa(\alpha)$ for state (14) vs T/T_C , for gap parameter $\Delta\Lambda/v=0.6$ and impurity scattering rate $\Gamma/\Delta_0=0.2$ (solid curve) and $\Gamma/\Delta_0=0.5$ (dashed curve).

6. Integrand in Eq. (8) for κ_s/κ_n (without the factor $\omega^2 \text{sech}^2(\omega/2T)$) and no directional factor for heat flow (corresponding to YCBO) vs reduced frequency $\Omega = \omega/\Delta$ for state (14) and gap parameter $\Delta\Lambda/v=0.6$, for field direction $\alpha = 0$ (solid curve) and $\alpha = \pi/4$ (dashed curve). The impurity scattering rate is $\Gamma/\Delta_0=0.2$.

Fig1

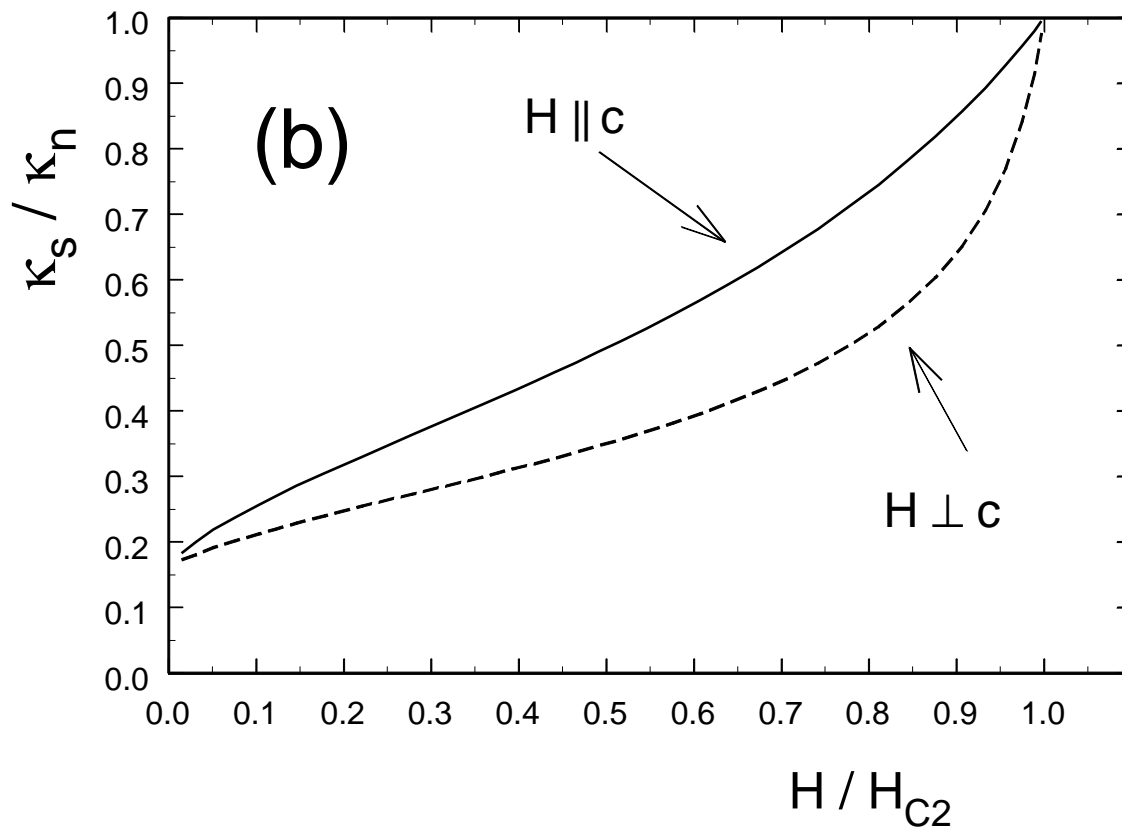
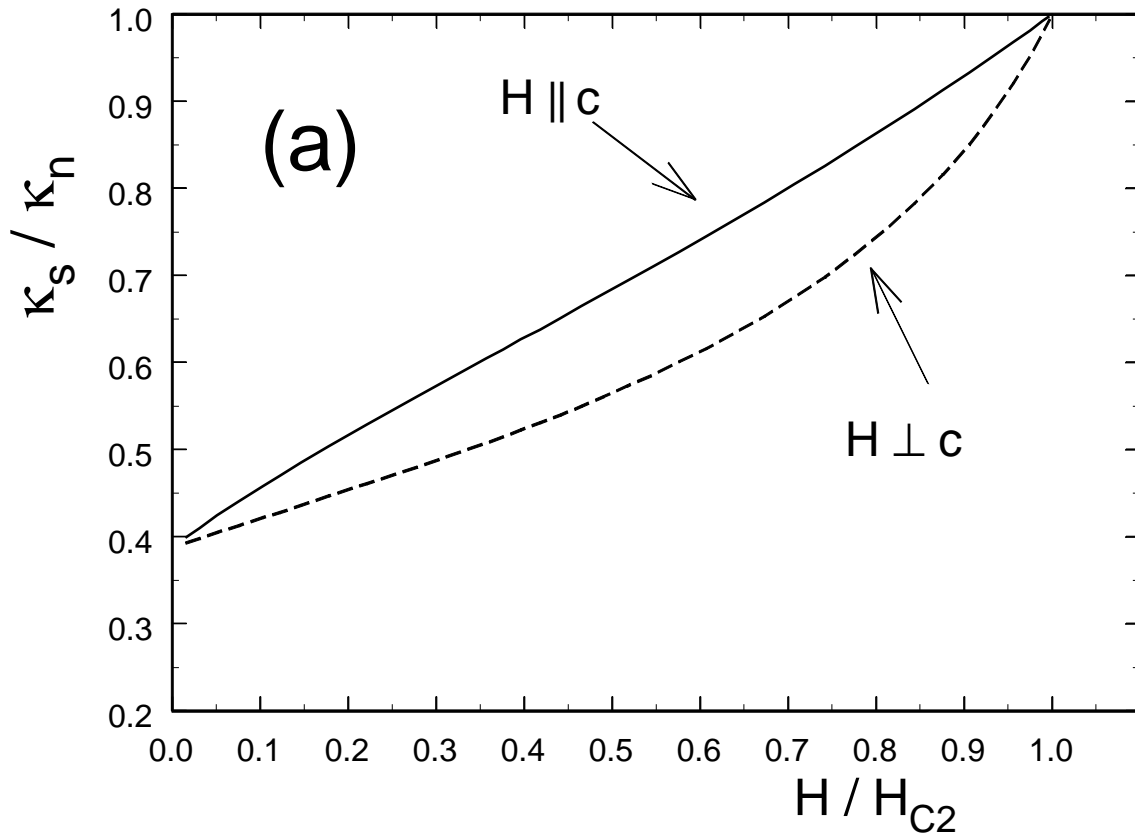


Fig. 2

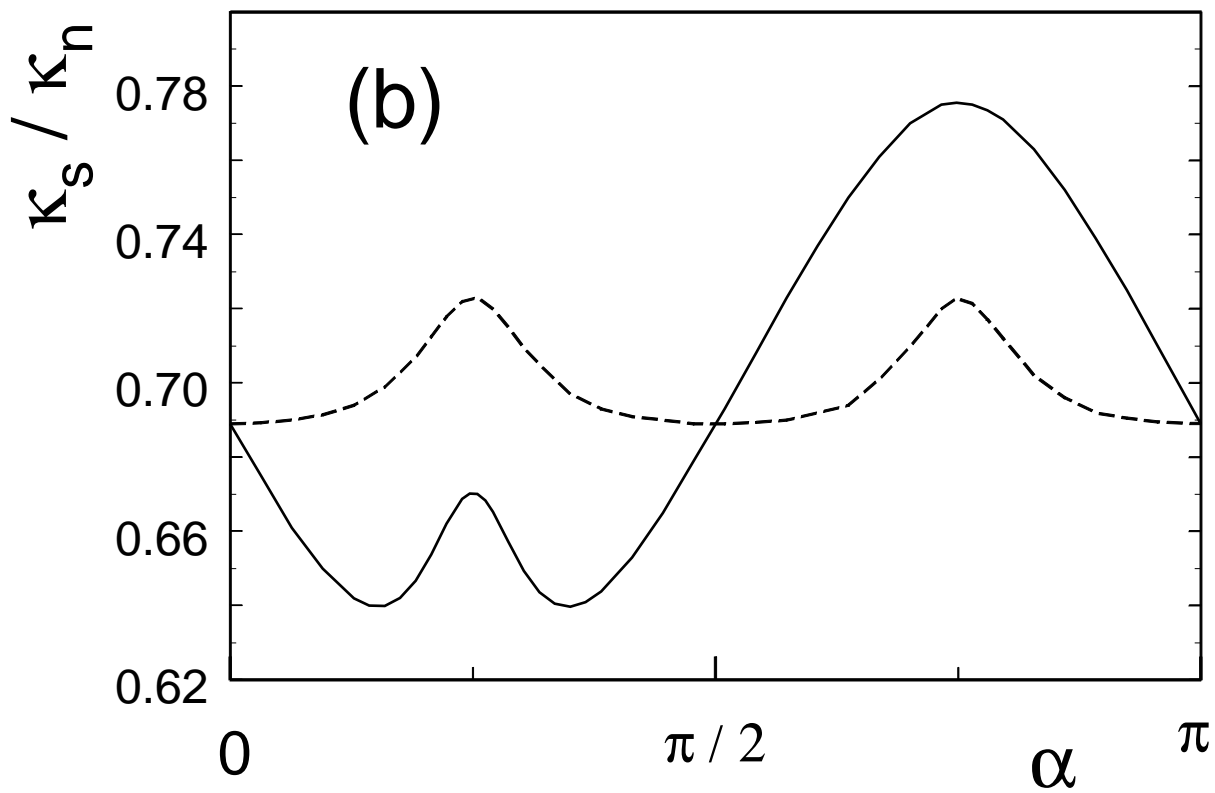
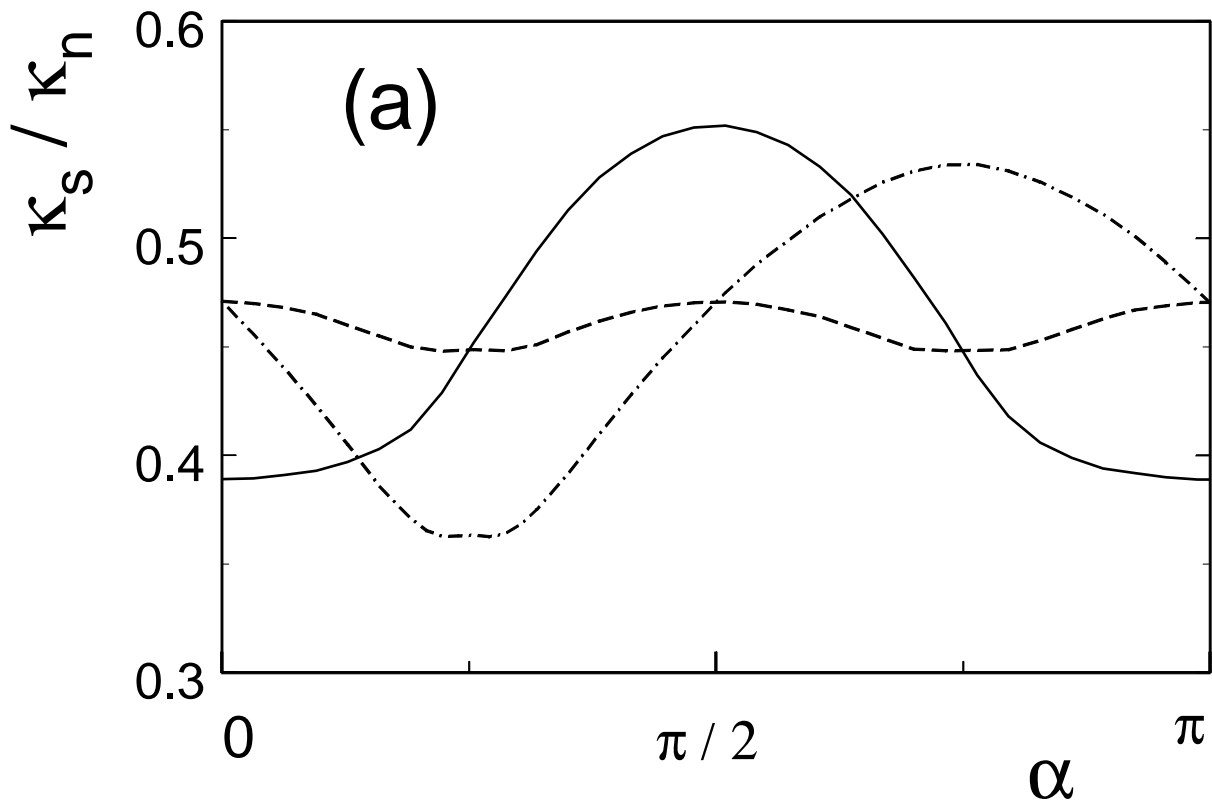


Fig. 3a

Fig. 3

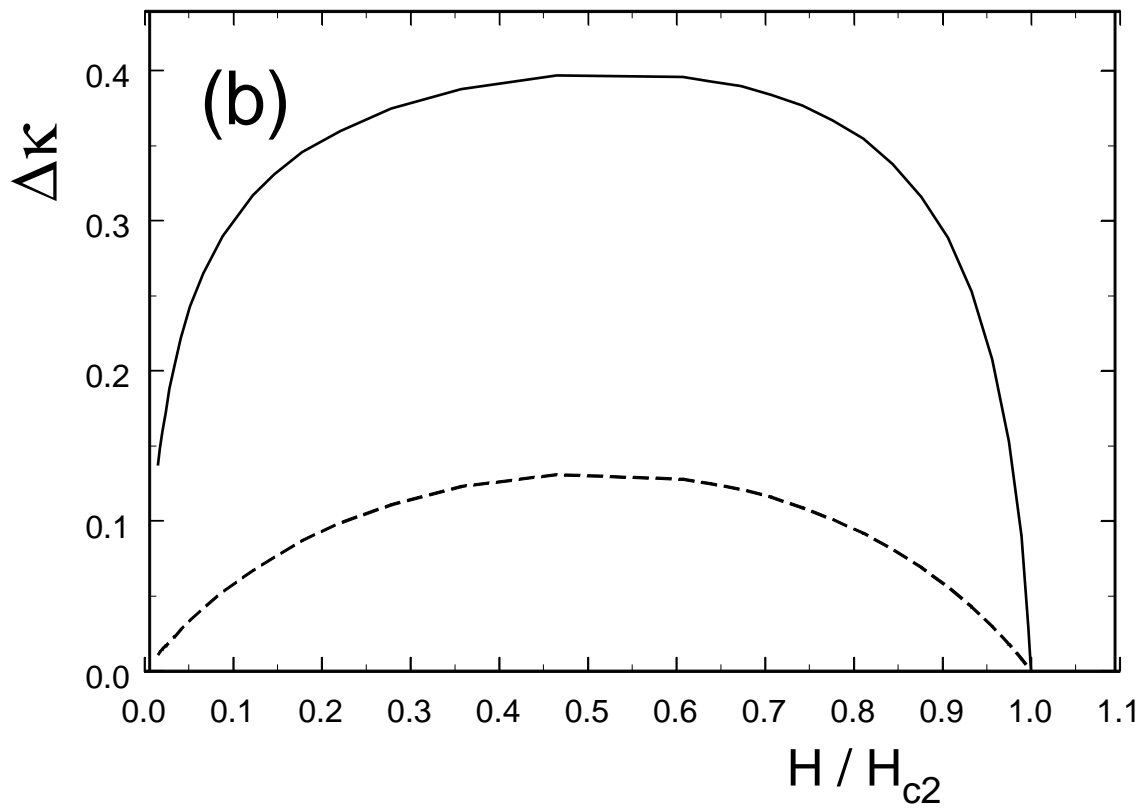
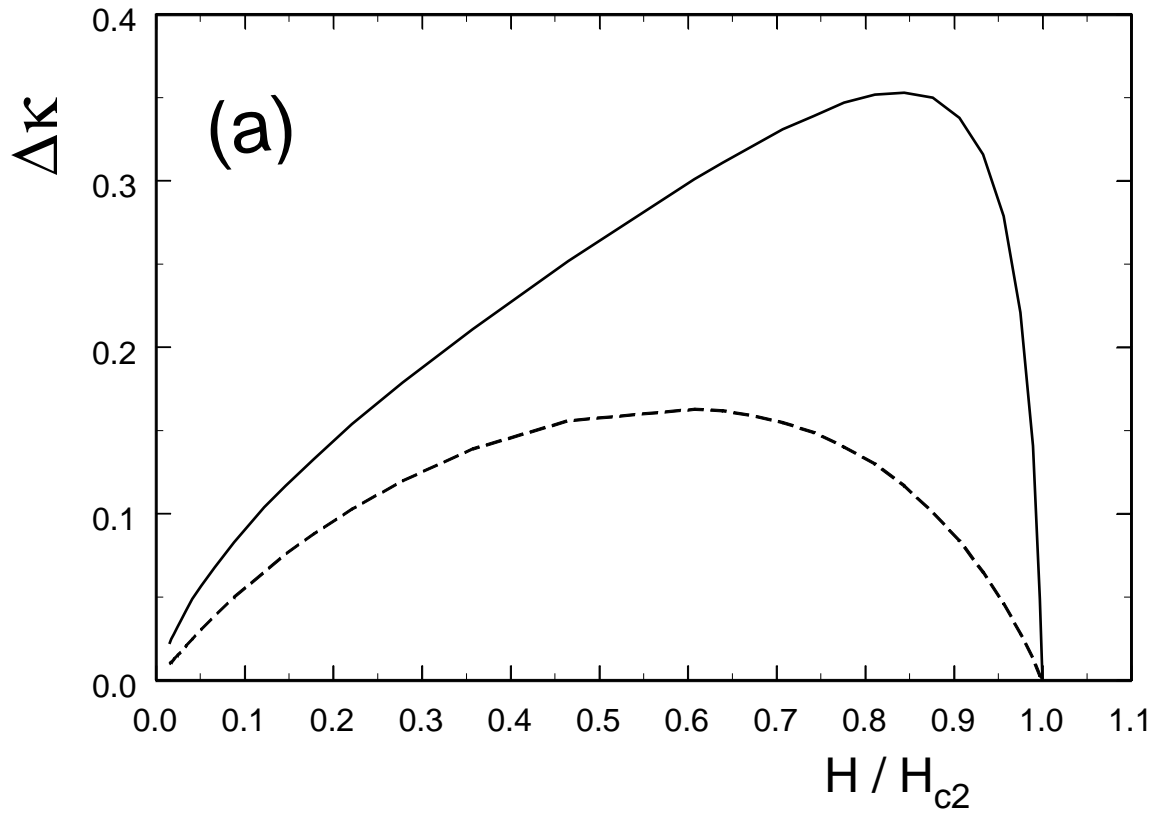


Fig. 4

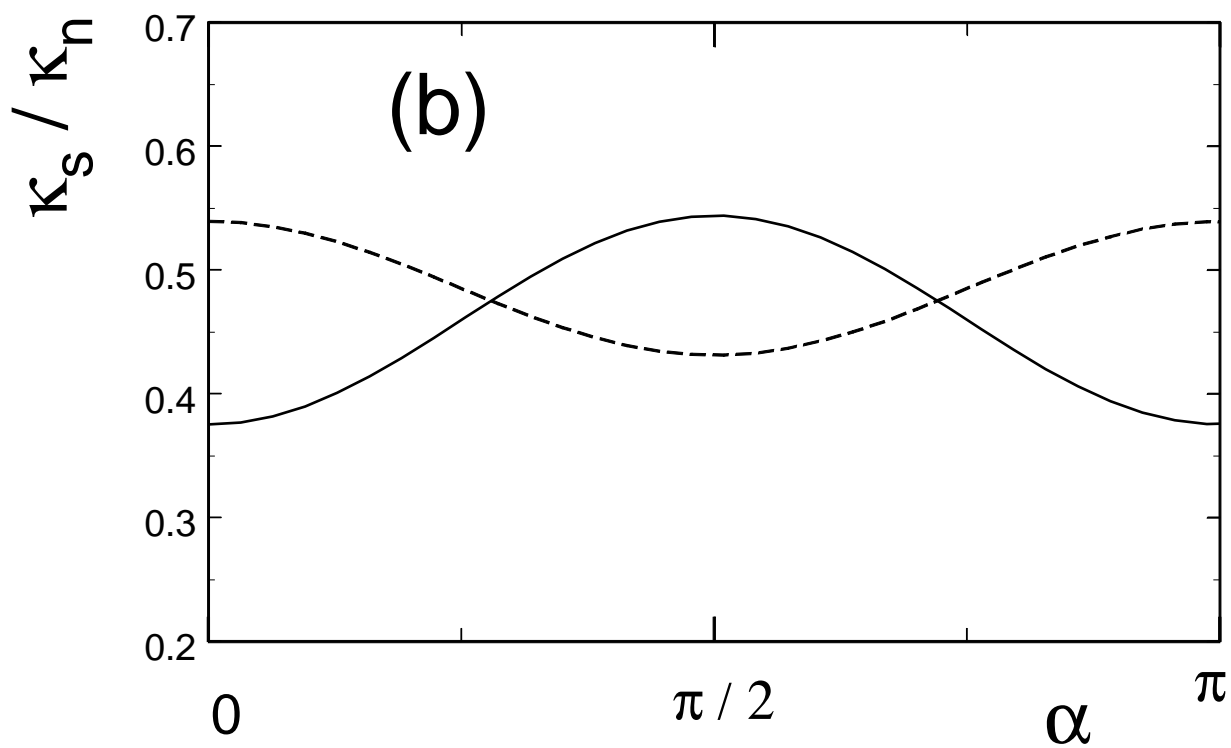
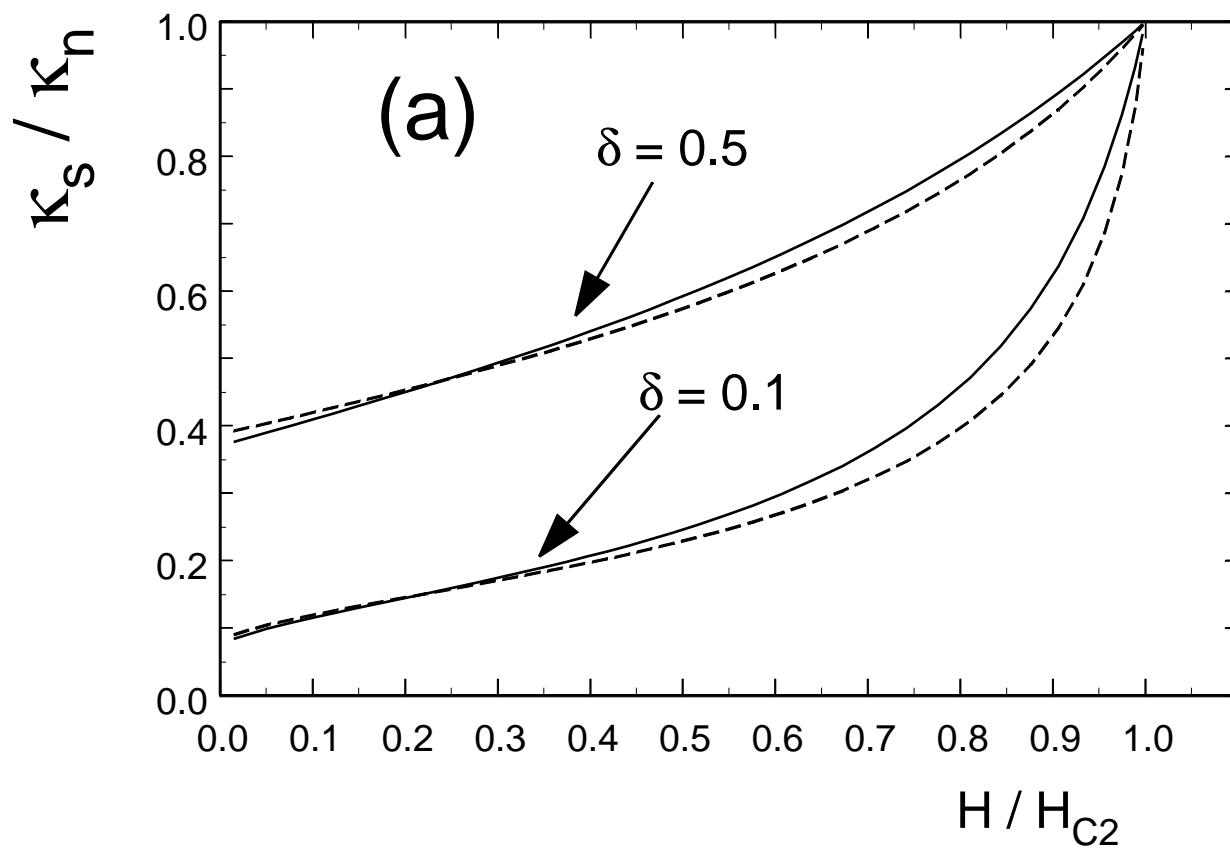


Fig. 5

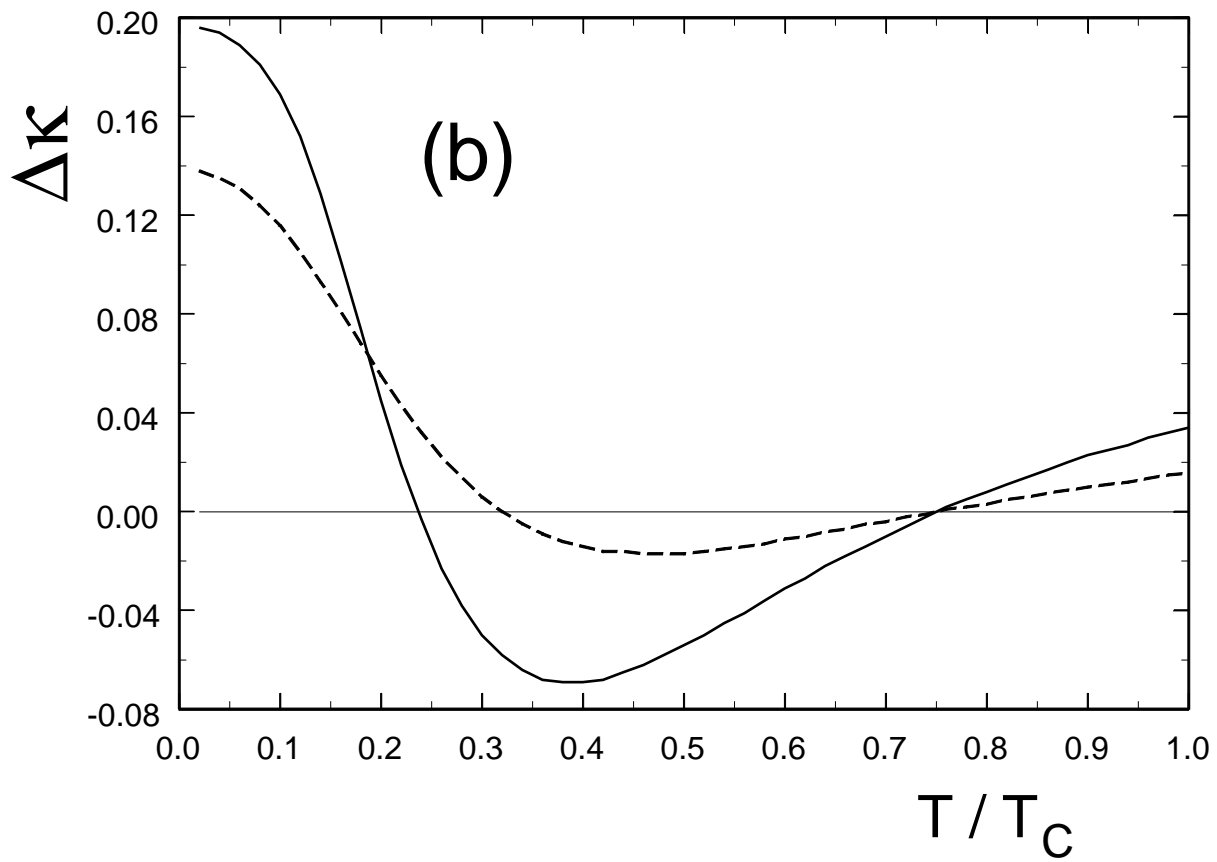
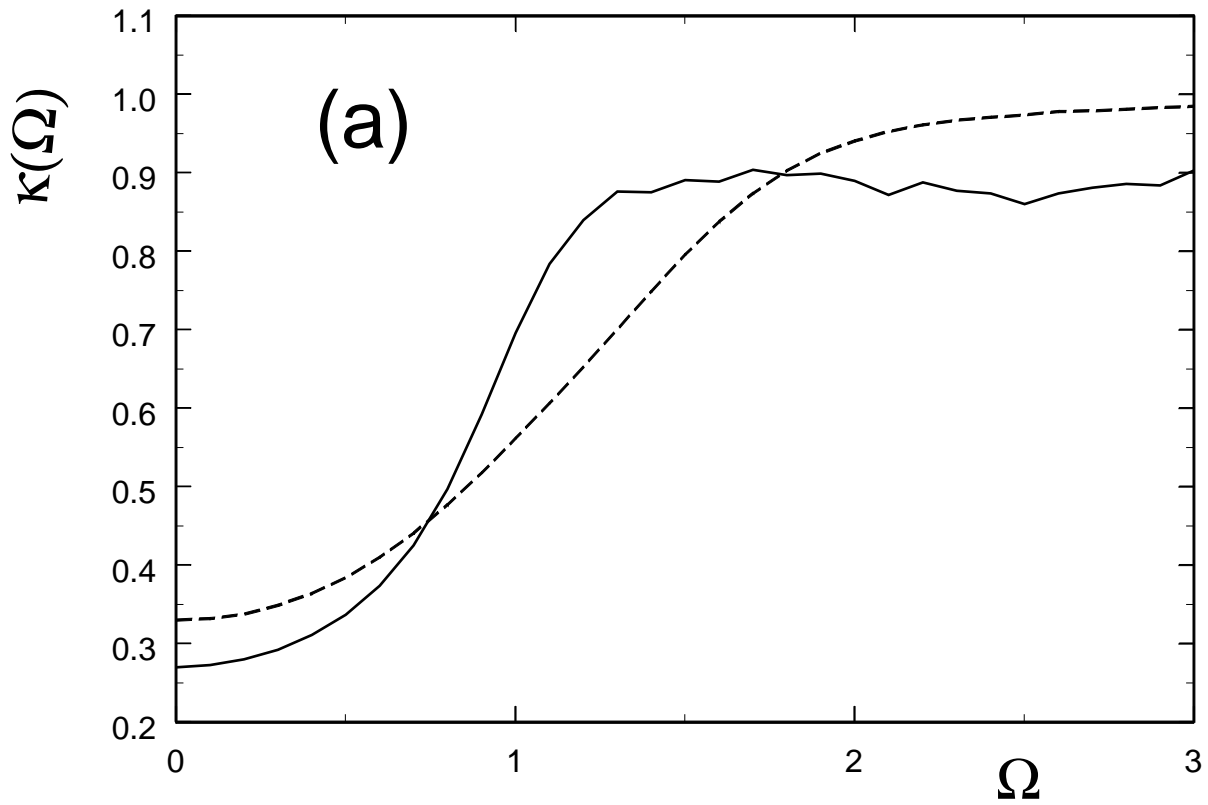


Fig.6

Fig. 6

